SH.3.6.06

Atmospheric Gamma-Ray Lines Produced by Cosmic Rays and Solar Energetic Particles

G.H. Share[1], R.J. Murphy[1], and E. Rieger[2]

[1] *E.O. Hulburt Center for Space Research, Naval Research Laboratory, Washington, DC 20375, USA*

[2] *Max Planck Institute for Extraterrestrial Physics, Garching, 85740, Germany*

Abstract

We describe observations of atmospheric γ rays produced by interactions of both cosmic rays and solar-energetic particles. The quiescent atmospheric spectrum produced by cosmic radiation was accumulated by the *Solar Maximum Mission (SMM)* spectrometer over its full 9-year lifetime. These observations are compared with a remarkable event observed by the spectrometer at about 1600 UT on 1989 October 20 during an intense solar energetic particle event at the Earth. The particle event followed an intense X-ray flare and coronal mass ejection that had occurred on the previous day. Twenty-three line features were identified from this event and twenty four were observed from the quiescent atmosphere. We compare the energies, widths and intensities of the different lines in both these spectra and discuss their origins.

1 Introduction:

The Earth's atmosphere is by far the most intense source of γ radiation observed by satellite-borne spectrometers. Energetic protons in the cosmic radiation and in solar energetic particle events interact with nuclei in the atmosphere to directly excite nuclear states, create spallation products in excited states, and produce secondary neutrons. These neutrons also excite nuclear states and produce spallation products. Letaw et al. (1989) listed the most intense γ-ray lines from these processes based on earlier compilations by Ling (1975), Ramaty, Kozlovsky, and Lingenfelter (1979), and nuclear data tables. Comprehensive nuclear-line observations of atmospheric γ rays produced by cosmic-ray interactions have been conducted using NASA's *HEAO 3* high-resolution (Mahoney, Ling and Jacobson 1981; Willett and Mahoney 1992) and *SMM* moderate-resolution (Letaw et al. 1989) spectrometer experiments.

2 Observations:

The spectrum of atmospheric γ rays was derived by using data accumulated in 10.4×10^6 s over a 9-year period with the instrument's axis pointed to within 72° of the center of the Earth. This spectrum contains instrumental background lines in addition to atmospheric radiation produced by cosmic-ray interactions. Letaw et al. (1989) demonstrated how most of the instrumental radiation can be eliminated by making a time-normalized subtraction of spectra with the instrument axis pointing away from the Earth. This subtraction was done for each orbit in order to minimize systematic effects. The background-subtracted spectrum is moderately distorted because atmospheric radiation leaking into the sky-viewing data is subtracted from the spectrum and this leakage is energy dependent; it varies from ~20% at 0.3 MeV to ~50% at 5 MeV. We corrected for this energy-dependent effect and plot what we call the 'quiescent' atmospheric spectrum in Figure 1. The positron annihilation line at 0.511 MeV and its atmospherically scattered Compton continuum dominate the spectrum between ~0.3 and 0.55 MeV. A bremsstrahlung continuum and various nuclear line features dominate the spectrum at higher energies.

We also plot the spectrum observed from 15:50:52 to 16:05:04 UT on 1989 October 20 during the period of high geomagnetic disturbance that followed an intense class X13 X-ray flare and coronal mass ejection on the previous day. The atmospheric emission increased about 40-fold during this time interval and was dominated by annihilation and nuclear line emission. The latter is evidenced by the precipitous fall-off in rate above ~7 MeV where the nuclear contribution ends and contrasts with the strong continuum at these energies observed in the quiescent spectrum. Most of the line features in the quiescent spectrum are more strikingly evident in the solar event spectrum. Upon close inspection the features in the solar event spectrum are slightly shifted (~1%) to lower energy. This shift is purely instrumental and is due to the active gain-control system used by the spectrometer. The nuclear lines in the solar-event spectrum are much more intense relative to the annihilation line, its scattered continuum, and the bremsstrahlung than they are in the quiescent spectrum. This is due to the softer proton spectrum of solar energetic particles compared with that of the cosmic radiation.

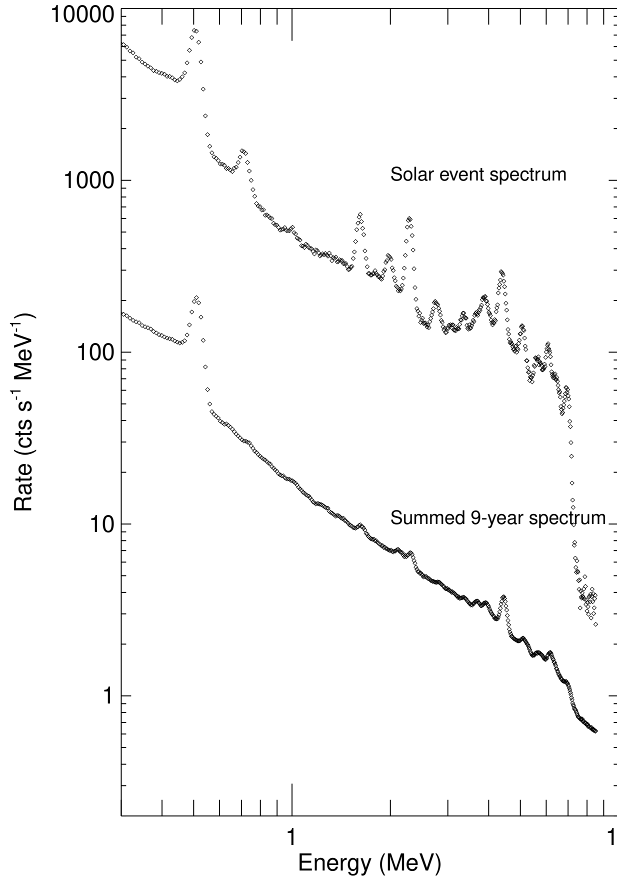

Figure 1: Comparison of the quiescent atmospheric spectrum, produced by cosmic rays observed over 9 years, with the spectrum excited by the 1989 October solar energetic particle event.

3 Nuclear Line Fits:

Both spectra contain over twenty line features above the annihilation line superimposed on a bremsstrahlung continuum that hardens with energy. This continuum is represented by the sum of two power laws. We used an iterative approach in fitting these spectra over the energy range from 0.65 to 8.5 MeV. Our goal was to fit simultaneously for all the constants and indices of the power laws and the energies, widths, and fluxes of the lines. This procedure is inherently unstable with so many free parameters. In order to accomplish this, we initially fixed the energies and widths of the lines and then incrementally freed these parameters for individual lines, starting from the highest energies and working down. The fitted energies and widths (FWHM) for the lines in the quiescent and solar event spectra are listed in Table 1. The fifth column is the quiescent/solar event flux ratio, normalized to the ratio for the 2.313 MeV line from ^{14}N. The line energies for the solar event have been corrected by the 1% instrumental shift determined by comparing the best-fit energies for the two strong and resolved ^{14}N de-excitation lines at 1.635 and 2.313 MeV with their laboratory values. The errors in line energy and width include statistical and systematic uncertainties in the fits in addition to limitations in knowledge of the energy-to-channel calibration and instrumental line broadening. We list possible line identifications ordered by energy for both spectra in the last column. We performed a separate fit from 0.57 to 0.97 MeV to obtain parameters of the ~0.65 and 0.73 MeV lines in the quiescent spectrum.

We also separately fit both spectra from 0.35 to 0.62 MeV with an incident photon model containing a single power law, the annihilation line, and its Compton continuum from scattering in the atmosphere. The fluxes in Compton-scattered annihilation radiation above 0.3 MeV are 1.62 ± 0.03 and 0.047 ± 0.001 γ cm^{-2} s^{-1} for the solar event and quiescent spectra, respectively. Comparing these fluxes with the annihilation line fluxes we find that the scattered/line flux ratios are 1.26 ± .03 and 1.37 ± .02 for the solar event and quiescent spectra, respectively. From this comparison we see that the Compton-scattering depth for the solar energetic particle spectrum is less than for the cosmic-ray quiescent spectrum. This is expected because the

TABLE 1

COMPARISON OF SMM ATMOSPHERIC LINE OBSERVATIONS

Energy, keV		Width (FWHM), keV		Quiescent/Solar	Identification (keV)
Quiescent	Solar Event	Quiescent	Solar Event	Flux Ratio	
513.4 ± 3.0	513.3 ± 3.0	13.0 ± 7.3	17.3 ± 5.5	10.07 ± 1.10	e^+-e^- annihilation line
652.6 ± 4.0		39.6 ± 16.7			^{14}C (613, 634)
733.9 ± 3.8	721.3 ± 3.1	10.6 ± 40.2	30.4 ± 5.2	1.16 ± 0.36	^{10}B (718); ^{14}N (728)
842.5 ± 3.3		126.4 ± 20.0			^{14}C (808)
1005.4 ± 3.5	1014.0 ± 4.5	76.8 ± 7.1	19.9 ± 29.0	12.57 ± 2.39	^{10}B (1022)
1230.0 ± 10.0	1442.5 ± 133.1	668.1 ± 50.0	476.3 ± 199.0		^{14}C (1248); ^{10}B (1436)
1636.1 ± 3.5	1633.4 ± 3.1	34.9 ± 16.7	41.3 ± 8.9	1.02 ± 0.14	^{15}O (1617); ^{14}N (1635)
1855.3 ± 146.0	1999.3 ± 3.7	705.9 ± 136.6	42.0 ± 22.4		^{11}C(2000); ^{15}N (1884, 2000)
2141.2 ± 4.8	2073.7 ± 57.8	94.2 ± 20.5	642.9 ± 359.1		^{15}O (2034); ^{11}B (2124);^{10}B (2154); ^{16}O (2190)
2311.2 ± 3.5	2314.6 ± 3.1	40.2 ± 20.5	47.5 ± 11.6	1.00 ± 0.15	^{15}N (2297); ^{11}B (2298); ^{14}N (2313); ^{13}N (2365)
2488.3 ± 137.0	2509.2 ± 17.5	720.5 ± 473.4	106.6 ± 150.4		?
2866.7 ± 64.8	2792.4 ± 5.8	257.7 ± 141.7	129.3 ± 20.3	5.31 ± 6.67	^{16}O (2741); ^{10}B (2868)
3108.7 ± 25.5	3091.2 ± 9.9	235.6 ± 128.1	234.5 ± 14.4	9.46 ± 7.96	^{13}C (3089)
3394.6 ± 25.0	3381.8 ± 7.4	264.7 ± 137.2	105.9 ± 36.4	12.58 ± 7.83	^{14}N (3378)
3688.8 ± 22.6	3699.1 ± 18.6	196.2 ± 81.7	218.4 ± 52.2	5.62 ± 3.21	^{13}C (3684)
3891.5 ± 38.1	3906.2 ± 16.6	181.2 ± 73.1	88.9 ± 77.7	8.40 ± 6.93	^{13}C (3853);^{14}N (3890)
4153.3 ± 14.5	4155.9 ± 33.0	199.8 ± 27.1	281.1 ± 110.8	6.07 ± 2.15	^{16}O (4140)
4451.2 ± 3.0	4442.5 ± 3.0	163.3 ± 7.4	167.1 ± 7.4	3.22 ± 0.36	^{12}C (4438); ^{11}B (4444)
4737.1 ± 8.2	4841.7 ± 8.6	242.2 ± 17.4	119.0 ± 29.0	3.32 ± 0.40	^{11}B (4666, 4739); ^{11}C (4803); ^{14}N (4912)
5134.7 ± 4.3	5130.4 ± 3.7	253.3 ± 9.2	153.9 ± 11.6	1.96 ± 0.22	^{14}N (5105); ^{15}O (5180)
5223.7 ± 25.0	5199.6 ± 7.1	1577.5 ± 100.0	1707.8 ± 16.0		several unresolved lines
	5827.1 ± 17.4		117.1 ± 62.8		^{14}N (5833); ^{11}B (5851)
6150.9 ± 3.8	6158.5 ± 3.8	96.6 ± 22.0	68.4 ± 31.5	2.09 ± 0.23	^{16}O (6129); ^{15}O (6176); ^{14}N (6203)
$6287.0 \pm --$	6342.0 ± 7.0	$394.8 \pm --$	549.0 ± 17.2		^{14}N (6203, 6422); ^{15}N (6322); ^{11}C (6337)
6960.5 ± 3.9	7039.3 ± 3.7	453.1 ± 8.0	273.4 ± 9.9	3.43 ± 0.38	^{16}O (6917, 7117); ^{14}C (7010) ; ^{14}N (7027)

solar energetic particle spectrum is typically softer than the cosmic-ray spectrum. Letaw et al. (1989) estimated the quiescent depth to be ~21 g cm^{-2}.

In Table 2 we compare the *SMM* quiescent line measurements with those obtained by Willett and Mahoney (1992) using the high-resolution germanium spectrometer onboard *HEAO-3*. The line intensities observed by *SMM* and *HEAO-3* are in good agreement. The *SMM* instrumental width may be underestimated by 1 – 2 keV at 511 keV resulting in a 13-keV wide inferred width. The *SMM* line widths are generally broader than those measured by *HEAO-3*. The widths suggest Doppler-broadening ranging from about 1 to 3% for individually resolved lines. The *SMM* and *HEAO* line energies are in good agreement up to about 2 MeV and diverge somewhat at higher energies.

TABLE 2

COMPARISON OF SMM AND HEAO-3 LINE OBSERVATIONS

	Energy, keV		Width, keV		Flux, $10^{-4}\gamma$/cm^2-s-sr	
Lab	SMM	HEAO-3	SMM	HEAO-3	SMM	HEAO-3
511	513.4 ± 3.0	511.07 ± 0.1	13.0 ± 7.3	2.29 ± 0.3	87.3 ± 0.5	110.6 ± 2.2
1635	1636.1 ± 3.5	1634.8 ± 1.4	34.9 ± 16.7	20.2 ± 5.7	2.8 ± 0.2	3.4 ± 0.8
2313	2311.2 ± 3.5	2309.4 ± 1.9	40.2 ± 20.5	24.0 ± 5.4	5.3 ± 0.5	5.4 ± 0.8
3684	3688.8 ± 22.6	3673.0 ± 4.7	196.2 ± 81.7	70 ± 15	12.7 ± 6.7	4.0 ± 1.0
4444	4451.2 ± 3.0	4428.5 ± 7.5	163.3 ± 7.4	135 ± 12	22.8 ± 0.1	19.6 ± 2.1
5105, 5180	5134.7 ± 4.3	5090.2 ± 10.4	253.4 ± 9.2	95 ± 26	5.3 ± 0.1	3.4 ± 1.2
6129, 6170	6150.9 ± 3.8	6137.2 ± 10.2	96.6 ± 22.0	98 ± 27	4.0 ± 0.1	5.4 ± 1.5

Line features in the quiescent atmospheric spectrum generated by galactic cosmic rays are predominately the result of interactions by secondary neutrons (Ling 1995). In contrast, protons are likely to have produced the atmospheric spectrum observed during the solar event. As a result one would expect the quiescent atmospheric spectrum to contain ^{14}C de-excitation lines that are produced in the $^{14}N(n,p)^{14}C$ reaction. The quiescent atmospheric spectrum reveals features near ~0.65 and ~0.84 MeV which may be due to ^{14}C de-excitation lines; neither line is evident in the solar-event spectrum.

The ratios of quiescent/solar-event fluxes given in the fifth column of Table 1 are important in determining the line origins. They are normalized to the ratio observed for the 2.3 MeV ^{14}N de-excitation line. We expect other features that are dominated by direct excitation lines to have flux ratios close to unity. We also expect lines from spallation reactions to be more intense in the quiescent atmospheric than in the solar-event spectrum. A high ratio should therefore imply a feature dominated by spallation products. Flux ratios consistent with unity are found for the ^{14}N de-excitation lines near 0.73 and 1.63 MeV; the measured widths and energies of these lines are consistent with one another. All the remaining ratios are consistent with values in excess of unity and suggest contributions from spallation. We next compare a few of the atmospheric lines in the quiescent and solar event spectra to understand their origins.

<u>~1.0 MeV:</u> It is likely that this line comes from ^{10}B. The high flux ratio also suggests a spallation origin. The width of the quiescent line appears to be broader than that from the solar event.

<u>~1.9/2.0 MeV</u>: The solar-event spectrum reveals a line at 2.0 MeV having a Doppler broadening of ~2%. It is likely to be due to ^{11}C and ^{15}N. A much broader feature centered near 1.9 MeV appears to be required to fit the quiescent spectrum. The flux ratio is indeterminate.

<u>~3.4 MeV</u>: Both spectra reveal the presence of this line that is consistent with de-excitation of ^{14}N. The Doppler-broadened width of the line produced in the solar event is 3.1 ± 1.1 % and is consistent with those found for the lines at 1.63 and 2.31 MeV. The feature in the quiescent spectrum is broader and likely contains additional unresolved lines.

<u>~3.7 MeV</u>: Lines in both spectra are consistent in energy and width. They are consistent with de-excitation of ^{13}C, a spallation product. The Doppler widths are closer to ~5% and the flux ratio is not well determined, although it is also consistent with a spallation origin.

<u>~3.9 MeV</u>: This line is relatively well resolved from the line at ~3.7 MeV in both spectra. ^{14}N should be a major component and other lines, such as ^{13}C, may be responsible for the apparently larger width and higher flux in the quiescent spectrum.

<u>~4.4 MeV</u>: This is the strongest resolved nuclear-line feature. It is predominately from de-excitation of ^{11}B, although some contribution from ^{12}C is expected (Letaw et al. 1989). The measured widths in both spectra represent a Doppler broadening of 3 – 4%. This is larger than what is found for the ^{14}N de-excitation lines. The high quiescent/solar-event line flux ratio is reflective of its spallation origin.

<u>~5.1 MeV:</u> The 5.105 MeV line from de-excitation of ^{14}N is a likely source of the feature although some contribution from ^{15}O is expected, especially for the quiescent spectrum. The solar event line is Doppler broadened by ~3%. The flux ratio is ~2 and suggests that additional spallation lines such as ^{15}O contribute to the quiescent spectrum.

<u>~6.1 MeV</u>: The line energies in both spectra are higher than the 6.129 MeV expected for the first excited state of ^{16}O; this suggests a contribution from ^{15}O or ^{14}N. The broadening is ~1.5%. The flux ratio is also suggestive of spallation.

<u>~6.9 MeV</u>. De-excitation lines from ^{14}N and ^{16}O contribute, as well as the spallation product ^{14}C. The 4-6% Doppler broadening in the spectra also suggests contributions from more than one line.

This work was performed under NASA DPR W-18995.

References

Letaw, J.R. et al. 1989, JGR 94, 1211
Ling, J.C. 1975, JGR 80, 3241
Mahoney, W.A., Ling, J.C., & Jacobson, A.S. 1981, JGR 86, 11098
Ramaty, R., Kozlovsky, B. & Lingenfelter, R. 1979, ApJS 40, 487
Willett, J.B. & Mahoney W.A. 1992, JGR 97, 131